Effect of hemp on cement hydration: experimental characterization of the Interfacial Transition Zone

Fabien Delhomme, Elodie Prud'Homme, Clara Julliot, Tina Guillot, Sofiane Amziane, Sandrine Marceau

Effect of hemp on cement hydration: experimental characterization of the Interfacial Transition Zone

Fabien Delhomme[(1)*], Elodie Prud'homme[(2)], Clara Julliot[(1)], Tina Guillot[(1)], Sofiane Amziane[(3)], Sandrine Marceau[(4)]

[(1)] Univ. Lyon, INSA-Lyon, GEOMAS, EA 7495, F69621 Villeurbanne Cedex, France
[(2)] Univ. Lyon, INSA Lyon, MATEIS, UMR 5510, 7 Avenue Jean Capelle, 69100 Villeurbanne, France
[(3)] Université Blaise Pascal, Institut Pascal, Polytech Clermont-Ferrand, 63174, Aubière, France
[(4)] Université Gustave Eiffel, MAST/CPDM, 77454 Marne-la-Vallée Cedex 2, France

* Corresponding author; e-mail: fabien.delhomme@insa-lyon.fr

Abstract: Hempcrete is low carbon footprint building material, which consists in a mix of a cement and/or lime binder and vegetal particles (shiv). Its high porosity and low density give it good insulation, hygrothermal and acoustic properties. On the other hand, the mechanical strength of hempcrete is very poor, which limited its used like a filling material in a load bearing structure. Its limits mechanical properties are due, among other things, to an Interfacial Transition Zone (ITZ) around the shiv, which is not hydrated like the rest of the matrix. The identification of the size and the characteristics of this ITZ is a key parameter to improve the mechanical properties of these kind of bio-based material. A new experimental test protocol, based on image analysis, was developed to achieve repetitive and robust visual observations of the formation of the ITZ. The high-water absorption and the leaching of shiv are the main parameters, which drive the shape and strength of the ITZ. A microstructural characterization was also conducted to understand the nature and origin of this less hydrated zone around the hemp. This experimental protocol will allow to determine the mix parameters that impact ITZ development and select the most appropriate binder/vegetal fiber couple to use.

Keywords: Bio-based material; Interfacial Transition Zone; Hydration; Microstructural characterization; Infrared microscopy

1 Introduction

Hemp concretes are the most widely used biobased concretes in France. As an example, VICAT, one of the European leaders in the production of building materials, has developed a construction system composed of hemp shiv and Natural Prompt Cement. Although construction rules exist for these materials, their growth is still limited by the lack of knowledge and high variability of the performances of biobased concretes, especially for their mechanical properties [1]. In addition, even if it is not the main performance expected, they still require sufficient mechanical resistance to be unmolded, transported onsite, and handled. Several parameters, such as setting delays of the binder or potential degradation of plant particles have been identified to explain their mechanical weakness. Moreover, on existing buildings, problems of powdering of the materials in the core have been observed even when using binder/vegetal couples validated by the construction rules. Currently, while cementitious binders are well characterized [2, 3 ,4 ,5 ,6], the physico-chemical mechanisms that affect the setting of the binder in biobased concretes have not yet been well understood so far. The modification of the hydration of the binder is related to the extraction of compounds from the plant aggregates which are not chemically inert, contrary to the mineral aggregates of conventional concretes. As a consequence, empirical testing is currently used to assess the compatibility of specific biomass particles and binders couples. These tests validate the performance of a biomass batch and binder couple at a given time, but do not consider the important variability of plant chemical composition and microstructure. The latter depends for example on plant species, genetic material (genotype) and environment of its growth, but also on their transformation process. This lack of knowledge about the robustness and performance of plant-based concretes is the main obstacle to their development. Hempcrete offers a means of achieving the rules set by the French national environmental regulations (ER 2020), which applies since 2022, but also of improving technical aspects of the concrete used in construction today. When dry, hemp has a very low bulk density of around 110 $kg.m^{-3}$, meaning that hemp-based concrete is lightweight [7]. It is an effective insulation material with good hygrothermal and acoustic properties. It has low thermal conductivity (between 0.1 and 0.3 $W.m^{-1}.K^{-1}$, depending on the hemp/binder ratio and humidity) due to its porosity and low density [8]. That porosity and the hydrophilicity of hemp create a buffering effect [9] that regulates the humidity within the concrete. Hempcrete is also interesting from an ecological point of view, as it requires no pesticides and cleans the soil, leaving it in a better state than before. Furthermore, it reduces the distance and time of transport from the source to the building site since it uses materials cultivated locally. Finally, the plant particles in the hemp concrete act as a CO_2 trap during the lifetime of a building [10].

2 Literature review

Existing studies on biobased concretes formulated with mineral binders and vegetal aggregates from different origins and chemical compositions showed that the properties of materials are disparate. As an example, for identical formulations, the use of nine types of hemp shiv from different sources leads to differences in compression strength by a factor of 5, while the impact

on thermal conductivity is smaller [1]. These results are attributed to the particle size distribution of the bioresources, their water absorption and chemical composition and to the lixiviation of vegetal compounds.

About impact of vegetal components on the hydration of binders, some studies highlight the modification of the mechanisms and kinetics of hydration of mineral binders by vegetal components. Indeed, during the processing of plant-based concretes, vegetal compounds, such as polysaccharides and polyphenols extracted in the fresh concrete mixture, interact with the mineral phases. Some of these extracted compounds can slow down or even completely inhibit the setting of the binders. These results, observed with various vegetal concrete formulations containing wood, hemp, miscanthus, corn or sunflower, depend on the selected plant-mineral binder couple [7, 11, 12, 13, 14]. A correlation can be drawn between the biochemical nature of raw plant materials, including the plant cell wall quality (types, and relative sugars, phenolics, and lignin contents), the composition of the leachates, and the mechanical properties of bio-based concretes [11, 14].

Existing studies explain the impact of plants on the setting of mineral binders, citing two main mechanisms:

- The absorption of organic molecules on anhydrous cement grains, leading to the formation of a thin layer with low permeability surrounding them. Therefore, the limitation of water diffusion impedes or completely inhibits the hydration of the binder [12, 15]. This mechanism involves sugars. The impact of their nature and amount has been investigated in particular depth by Boix *et al.* [13].
- The capacity of some organic compounds to chelate Ca^{2+} ions [16], resulting in the formation of a Ca^{2+} complex which blocks the nucleation sites and prevents the growth of cement hydrates [14]. This mechanism is correlated with the presence of specific plant polyphenols – especially flavonoids [7]. To overcome these problems, treatments of the vegetal matter have been considered, such as lixiviation of the vegetal material with water or coating of the plant aggregates [13,17].

On a different scale of analysis, an interfacial transition zone (ITZ) is observed around the vegetal particles [7]. The ITZ is a gradual transition region where the composition and microstructure of the binder matrix are affected by the presence of the aggregate particles [18]. This impacts on the physical properties (workability, density, porosity, etc.), mechanical properties (compressive and tensile strength, modulus of elasticity, etc.), functional properties (hygrothermal insulation, sound absorption) and durability (drying shrinkage, resistance to freeze–thaw, etc.) of vegetal concretes [19]. In this study, a newly implemented protocol is set up using a hemp pellet put into a cement paste. The halo of less hydrated material created around this pellet is monitored using image analysis. Different analysis methods (infrared spectroscopy, infrared microspectroscopy, X-ray diffraction, thermodifferential and thermogravimetric analysis) have been used to characterize the hemp crushed for the pellet and to analyze the ITZ and the hydrated matrix.

3 Raw materials

The cement used to make up the cement paste is a Portland cement CEM I 52.2 R, kept at a temperature of 20°C in a sealed plastic bag. To reduce bleeding in the cement paste, KELCO-CRETE DG-F from BASF (Baden Aniline and Soda Factory) was used. This is a water-soluble biopolymer used in hydraulic cementitious systems as a viscosity modifying agent.

The characterizations of hemp were performed on sample dried at 50°C for at least 2 days, in accordance with the RILEM recommendations [20]. The hemp used for the experiments has a bulk density of 116 $kg.m^{-3}$. Its particle size distribution is extremely heterogeneous (Figure 1) [21] and the initial rate of absorption (1 min) is 135 % (Figure 2) [22].

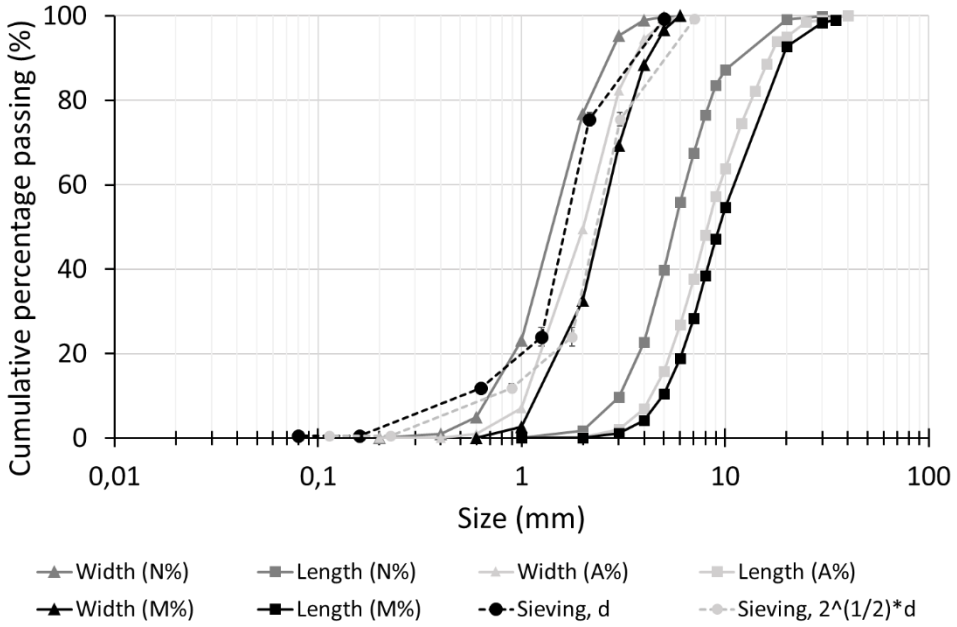

Figure 1. Particle size distribution of the hemp obtained by image analysis, considering both length and width of hemp (N%: Frequency distribution, A%: Area distribution, M%: volume distribution), or mechanical sieving (d: size of the aperture, 2^(1/2)d: size of the diagonal of the square aperture) [21].

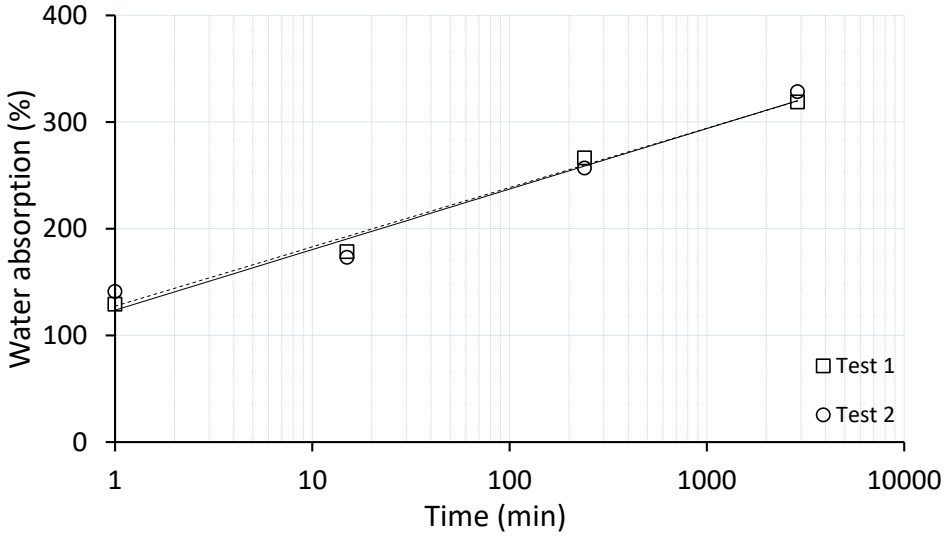

Figure 2. Water absorption of the hemp used [22]

4 Experimental techniques and protocols

4.1 Microstructural characterization techniques

A ThermoFisher Scientific iS50 device with Attenuated Total Reflection (ATR) mode was used for Fourier transform infrared spectroscopy measurements (FTIR). The spectra were acquired from 500 to 4000 cm^{-1}, with a digital step of 0.5 cm^{-1} (resolution 4) and on average, with 32 successive scans. Spectra were corrected between 1900 and 2400 cm^{-1} to remove CO_2 contribution, with an automatic baseline. The data were processed using OMNIC® software [23]. It was decided to differentiate the internal face (inside of the stem) from the external face (outside of the stem) of the shiv to see its influence. Hemp powder was also tested to investigate the regularity of the results and compare them with shiv.
X-ray diffraction (XRD) analysis was performed on a Brüker D8 Advance device directly on a pellet of constant size (13 mm in diameter and around 1 mm in diameter), which was made of 0.1 g of hemp ground and compressed at a pressure of 10 tons. After drying at 50°C, the pellet was removed from the oven and tested as soon as possible (approximately 10 min) to reduce the impact of water absorption due to air exposure, which can affect the results. The X-ray diffractograms were recorded between $2\theta = 5°$ to 70° with a step of 0.0305°. Data were analyzed using EVA software [24] with background and Kα2 corrections. Crystalline phases were identified by comparison with PDF (Powder Diffraction File) standards from ICDD (International Centre for Diffraction Data). A semi-quantification is made using EVA software, based on the evaluation of 9 crystalline phases identified by XRD: C2S (01-083-0461); C3S (01-073-0599); Anhydrite (01-072-0503); Calcite (01-087-1863); C3A (00-032-0150); Brownmillerite (01-074-1346); Portlandite (01-087-0673); Ettringite (01-072-0646); and Gypsum (00-036-0432).
Derivative Thermogravimetric Analysis (TGA) and Differential Thermal Analysis (DTA) is performed with a Labsys Evo (Setaram) on a 50 mg sample of hemp powder in an alumina crucible with a lid. The temperature ranges from 20 to 1000°C (heating rate: 10°C/min) under nitrogen (100 mL/min). The analysises are corrected using a blank, made of two empty crucibles with a lid. Data are processed with Setsoft software.
Infrared microspectroscopy (FT-IR mapping) is performed with a Nicolet iN10 infrared microscope (Thermo) using reflection mode. The spectra were produced with a total of 64 scans with a resolution 4.0 (digital step: 1.92 cm^{-1}); the atmospheric correction is a straight line from 2250 to 2400 cm^{-1}. The mapping uses 11284 spectra for a 2250×3075 μm^2 size. The investigation of the ITZ focused on the band relative to Portlandite at 3640 cm^{-1} and especially on the evolution of the area under this band, with a base line from 3660 to 3600 cm^{-1}. The data were analyzed using Specta Software.

4.2 Observation of ITZ

In order to study the ITZ between the hemp and the binder, the experiments were conducted on hemp pellets in contact with cement paste. The protocol was adapted and improved to tackle the issues encountered in previous studies like robustness, repeatability and accuracy, to

monitor the formation of the ITZ from the moment the binder is finished being poured. The compositions of the cement pastes used in this study are presented in Table 1.

Table 1. Mass of water and cement used to formulate the cement paste for one mold.

Ratios	W/C = 0.3	W/C = 0.4	W/C = 0.5	W/C = 0.6
Water (g)	240	300	350	390
Cement (g)	800	750	700	650

The protocol setup includes 5 steps:

1. Grind 1 g of dry hemp (stored at 50°C) in each of the two compartments of a planetary mill for 2 min (the four balls create a homogeneous result as seen in Figure 3). Then, form the 13 mm diameter pellets by compressing 0.1 g of hemp shiv at 100 kN in a manual hydraulic press.

Figure 3. Photos of 0.1g (a) raw hemp shives and (b) hemp after grinding.

2. Make the cement paste and pour it into the 60×160×35 mm^3 mold, covered with plastic film (Figure 4 (a)). Level.
3. Spray the glue onto the dry pellets and stick them onto an 8×8 cm^2 glass plate. Slowly press the glass plate, with the glued pellet, onto the cement paste, working from one side of the mold to the other.
4. Take a picture every 10 min in the first 24h, then every hour until 3 days (Figure 4 (b)).
5. Calculate the area of the ITZ by image analysis.

Figure 4. (a) Mold and plastic film to pour the cement paste and (b) pellet cast in cement paste after cement setting.

In order to obtain the final protocol and confirm its reproducibility, numerous tests were performed. The main issues encountered were gaps forming between the binder and the edges of the pellet, which prevents hydric and chemical transfers, and excessive bleeding, leading to the formation of a halo of irregular thickness with large growths, which cannot be exploited by image analysis. Different W/C ratios, setup methods (with or without vibrations, glue application and levelling) were tested, to achieve repeatable, sharp and regular halos without bleeding or gaps between the binder and the pellet (Table 2).

Table 2. Tests undergone to obtain the final protocol.

Test n°	Goal	Comment	W/C	Conclusion
1	Protocol setup	Pour cement paste first	0.5	20×10cm glass: gap 10×10cm glass: no gap
2		Individual glass plates Variation of W/C	0.5 and 0.4	Manifestation of an extension
3		Reduce bleeding	0.4 and 0.5 + Diutan Gum	Extension for W/C =0.4 No extension and reduced halo for W/C=0.5 + Diutan Gum
4		Glue test	0.5	Glue on the pellet at 20 cm
5		Confirm glue test	0.5	Weight applied to stick the pellet
6		Vibration and levelling	0.5	No vibration and levelling work better
7		Confirm final protocol	0.5	Protocol confirmed
8	Influence of W/C	Variation of W/C	0.3 and 0.6	Limits of the protocol reached
9		Variation of W/C	0.3 and 0.6	Limits of the protocol reached
10		Overnight video acquisition	0.5	Monitoring the formation of the ITZ in black and white every 10 min
11		Overnight video acquisition	0.5	Monitoring the formation of the ITZ in color every 5 min

The formation of the ITZ was monitored by imaging with two types of cameras:

- For the overnight acquisition, the software Labview [25] was used, with an adjustable time step. For the black and white acquisition, the model of camera used was a Stingray F-201B/F-201C with a Sony Super HAD CCD ICX274 sensor running at 14 frames per second at full resolution. The pixel size is 4.4×4.4 µm². The diaphragm is set at 3.

- For the color acquisition, the camera was a mvBlueFOX3-2 2071a with a Sony IMX428 sensor. It has a 3216×2208 resolution and pixel size of 2.4×2.4 µm². The diaphragm is set on 4 since the sample became too saturated during the black and white test.

Table 3. Summary of the tests to compare the ITZ and the hydrated matrix.

Test n°	Method	Number of samples	Type of sample	W/C
1	FT-IR analysis	3	ITZ Hydrated matrix Anhydrous cement	0.5
2	FT-IR mapping	1	Pellet still in the cement	0.5
3	XRD	8	4 ITZ 4 Hydrated matrix	0.5
4	XRD	4	2 ITZ 2 Hydrated matrix	0.3
5	DTA	2	ITZ Hydrated matrix	0.5
6	DTA	2	ITZ Hydrated matrix	0.3

5 Results

5.1 Raw material characterization

The characterization of hemp shives by thermal analysis reveals two exothermic phenomena with maximum values at 329°C and 403°C (Figure 5). The first can be attributed to the thermal depolymerization of hemicelluloses and pectin. The second is related to cellulose decomposition. Once the hemicellulose and pectin were destroyed, the degradation of lignin continues throughout the burning and the decomposition of cellulose [26]. After heat treatment, the total mass loss is 96.2%, and only 3.8% of the initial hemp is recovered as ash.

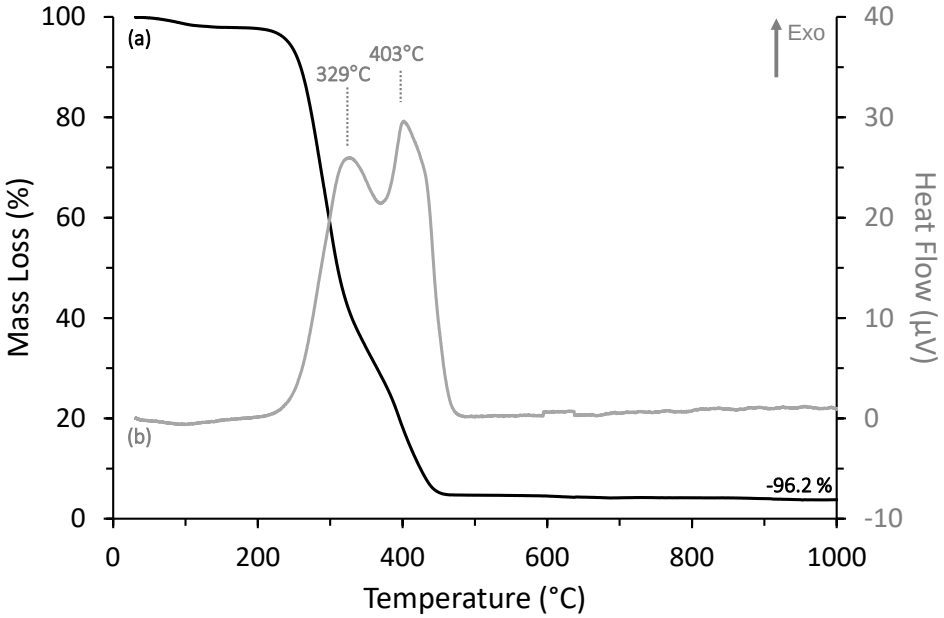

Figure 5. (a) TGA and (b) DTA of the hemp.

As expected, FTIR analysis demonstrates the presence of polysaccharides (3340, 2910, 890 cm^{-1}), hemicellulose (1740, 1180-930 cm^{-1}) cellulose (1400-1180 cm^{-1}) and lignin (1240 cm^{-1}) (Figure 6) [26]. The investigation of the difference in composition between the internal and external faces of the particle does not reveal any significant differences in terms of the positioning of the vibration bands (Figure 6 (a) and (b)). However, differences in absorbance ratios between bands are seen, especially for cellulose and hemicellulose, which could reflect a difference of cellulose crystallinity between the inside and the outside of the shive [27, 28]. The use of a pellet composed of crushed shives averages these differences and minimizes the impact of these heterogeneities depending on the side of the hemp from which the particle originates (Figure 6 (c)). These analyses are important because during tests in the presence of cement, the use of ground hemp pellets will offer an overall view of the behavior with a more homogeneous raw material than with the unprocessed particles.

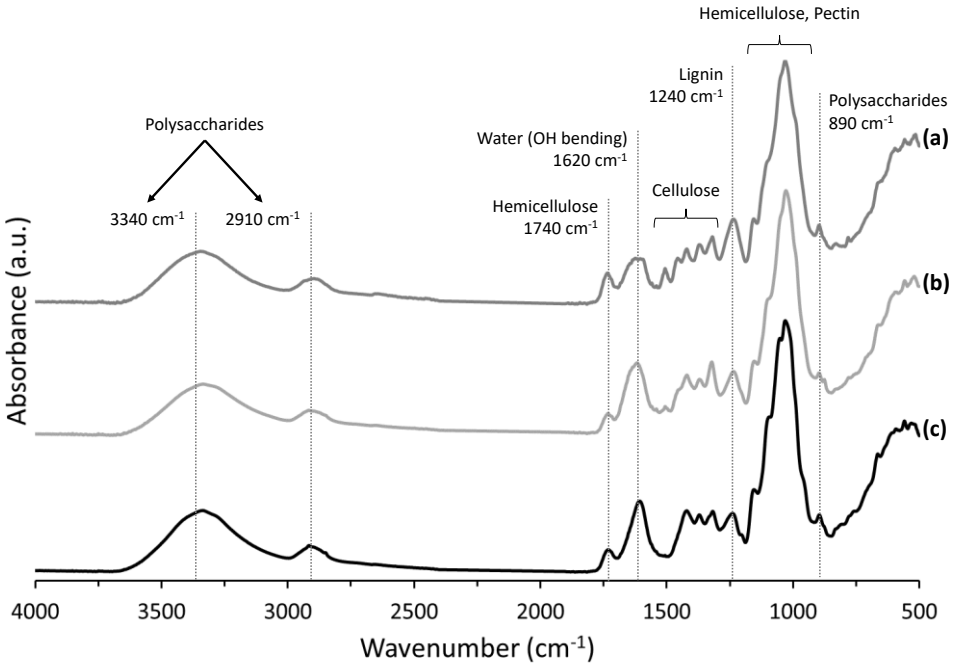

Figure 6. Infrared spectra of (a) the internal and (b) the external face of hemp shive, and (c) hemp powder after grinding in a planetary mill.

5.2 Observation and characterization of the ITZ

The overnight data acquisition showed the formation of the ITZ. First, the pellet absorbs the water in the cement paste (Figure 7). Then it begins to dry, and the ITZ forms from its outer edges after approximately 5 h. The cement paste slowly becomes lighter in the vicinity of the pellet. The extracts of hemp seem to be released as soon as the pellet is placed into the cement paste, and percolate around the pellet over a distance of few millimeters. Then, the paste begins to set from the edges of the mold to the pellet, and the halo appears due to the presence of chemical components which delay or interfere with the setting.

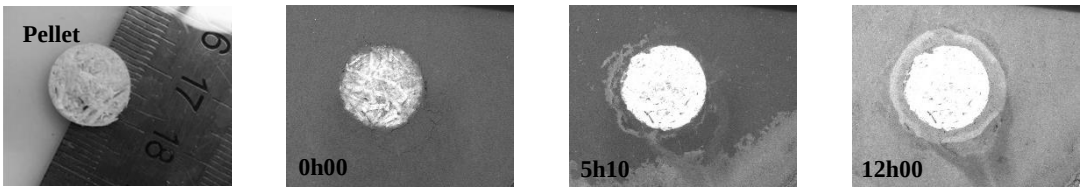

Figure 7. Video acquisition at different times: t=0 s, t=5h10 (formation of the halo from the edges), t = 12 h (complete halo formed).

FTIR spectra of cement (Figure 8) show that while similarities can be found between the ITZ and the hydrated matrix in terms of the microstructural composition, like the presence of portlandite (3642 cm^{-1}) and O-H bending in cement hydrates (in the 3400 cm^{-1} region), certain components are also in common with the anhydrous cement, like the presence of gypsum (1140 cm^{-1}), alite, belite, and anhydrite.

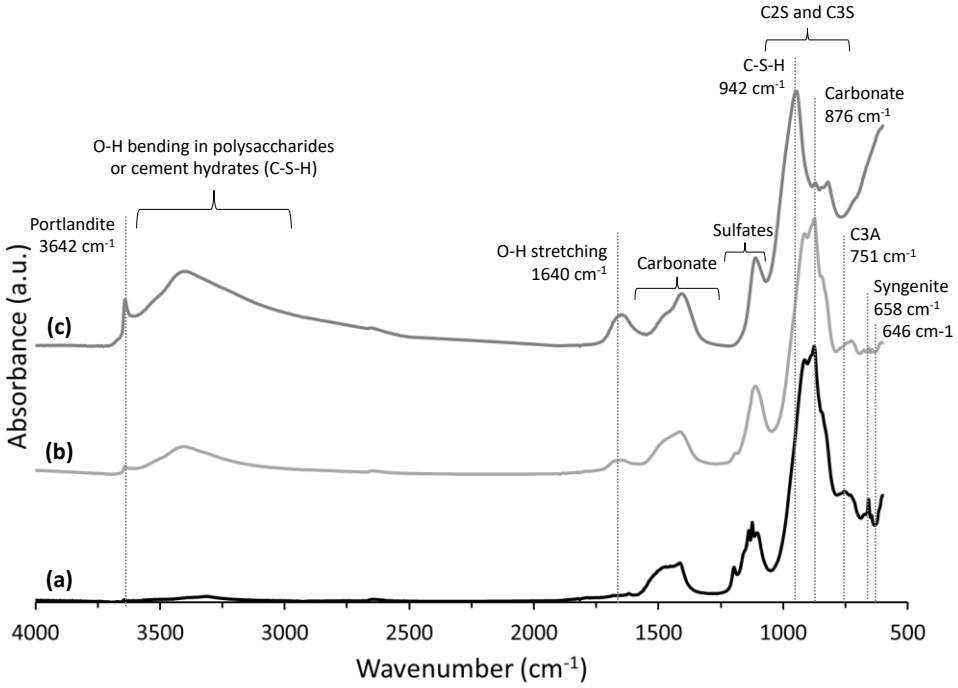

Figure 8. Infrared spectra of (a) anhydrous cement, (b) the matrix with W/C=0.5 and (c) the ITZ.

FTIR mapping (Figure 9 (a)) shows the evolution of the area under the band relative to portlandite at 3640 cm^{-1}, with a base line from 3660 to 3600 cm^{-1}. Portlandite is chosen because it partially reflects the hydration of the cement. The color scale of the mapping ranges from blue, showing a very small vibration band area, through green, to red, highlighting a larger vibration band area. The lower part of the map corresponds to the area near the hemp pellet, as evidenced by the observation (Figure 9 (b)). The gradient from green to red clearly shows a gradient of Portlandite concentration from the least concentrated in the ITZ to the most concentrated in the matrix. This clearly demonstrates the low hydration of the ITZ compared to the rest of the cement matrix. This type of observation helps define the ITZ and will allow researchers, in future studies, to compare the effect of different binders or fibers on the ITZ from a chemical point of view. Note that the blue part of the map corresponds to a problem of planarity of the sample – thus, the apparatus was unable to focus in this area, making the spectra

of this zone invalid. This problem is due to the sample holder blocking the sample without the possibility of adjustment, and could be corrected in future studies by using a sample holder with an accurate adjustment.

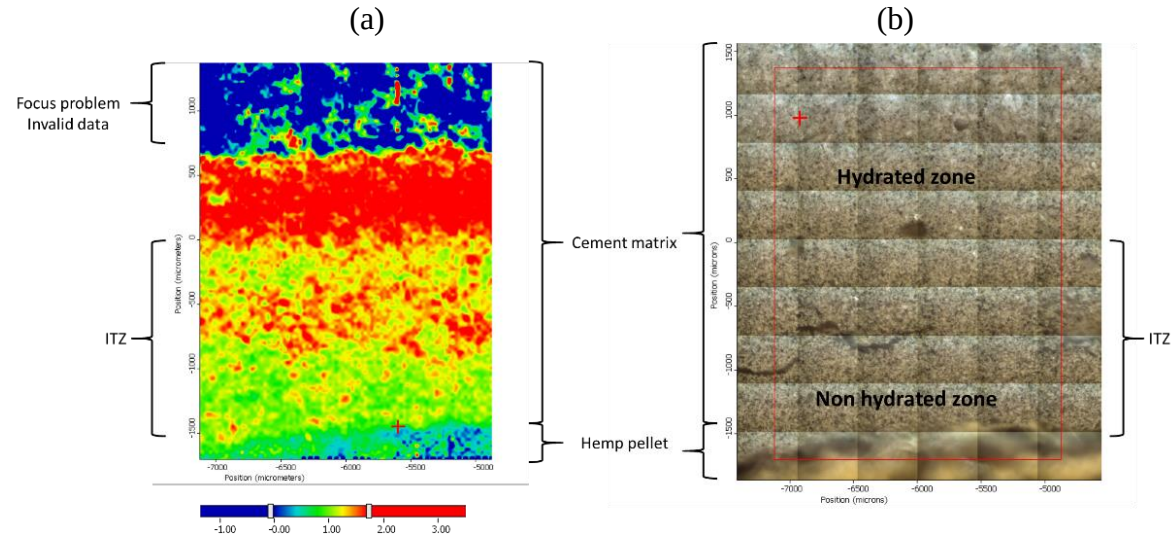

Figure 9. (a) Infrared mapping and (b) zone observed of the vibration band area relative to Portlandite (3640 cm^{-1}) of a W/C=0.5 sample.

The semi-quantitative analysis on both the ITZ and the hydrated matrix through XRD analysis for a W/C=0.5 sample (Table 4) shows a drastic difference in the relative quantities of Portlandite and C_3S that are characteristic of the hydrated and anhydrous phases respectively. DTA and TGA corroborates this analysis, since the hydrated matrix displays a significant endothermic reaction around 125°C (Figure 10 (a)) and a huge mass loss between 30 and 200°C, corresponding to C-S-H dehydroxylation (Figure 10 (b)). Another mass loss occurs between 400 and 600°C, coupled with a second endothermic reaction around 489°C on the heat flow, that corresponds to the degradation of portlandite. Neither of these phenomena is observed in the ITZ. Consequently, the ITZ, visually observed, is also distinguishable chemically as well by a lack of hydration.

Table 4. Semi-quantitative analysis for W/C=0.3 and W/C=0.5 using XRD analysis.

Component	W/C	Evaluation in the matrix (%)	Evaluation in the ITZ (%)
Portlandite	0.3	31.2	3.1
	0.5	37.2	6.6
C_3S	0.3	16.9	53.9
	0.5	9.6	57.2

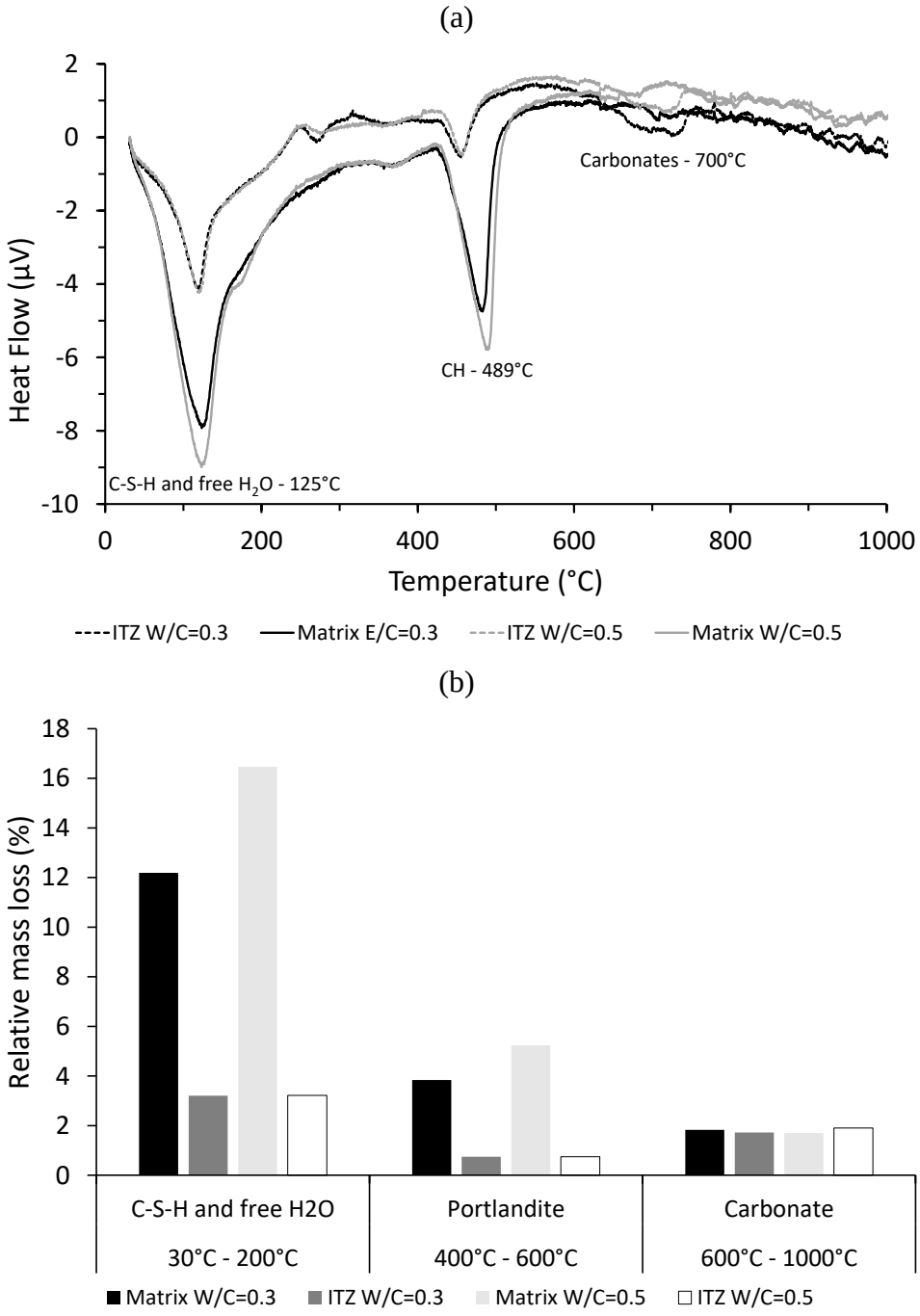

Figure 10. (a) Heat flow and (b) mass loss calculated from TGA analysis related to C-S-H, Portlandite and Carbonate for ITZ and the matrix, for a water-to-cement ratio of 0.3 and 0.5.

5.3 Influence of W/C ratio on the ITZ

The impact of the quantity of water on the ITZ was studied through two cement pastes with ratios of 0.5 or 0.3. While the chemical components are the same for W/C=0.3 and W/C=0.5 ratios, their quantities are different. The semi-quantitative analysis revealed that W/C=0.3 samples contained 15% and 53% less Portlandite in the matrix and in the ITZ respectively. This is consistent with the less significant mass loss corresponding to C-S-H and portlandite in the W/C=0.3 sample (Figure 10). Similarly, the amount of anhydrous C_3S is higher with a lower

W/C ratio. The samples obtained throughout the tests summarized in Table 3 were analyzed by image analysis to calculate the areas of the ITZ (Figure 11). The less viscous the paste is, the easier the extracts can diffuse and delay the hydration, creating a larger ITZ. With the binder used, the W/C ratio must be kept between 0.3 and 0.6 which are the limiting values for the test using the protocol developed in this study. Indeed, to be effective, this test requires perfect coverage of the pellet, which is not the case when the paste is too plastic. It is also essential to avoid bleeding of the cement paste, which can occur when the paste is overly fluid.

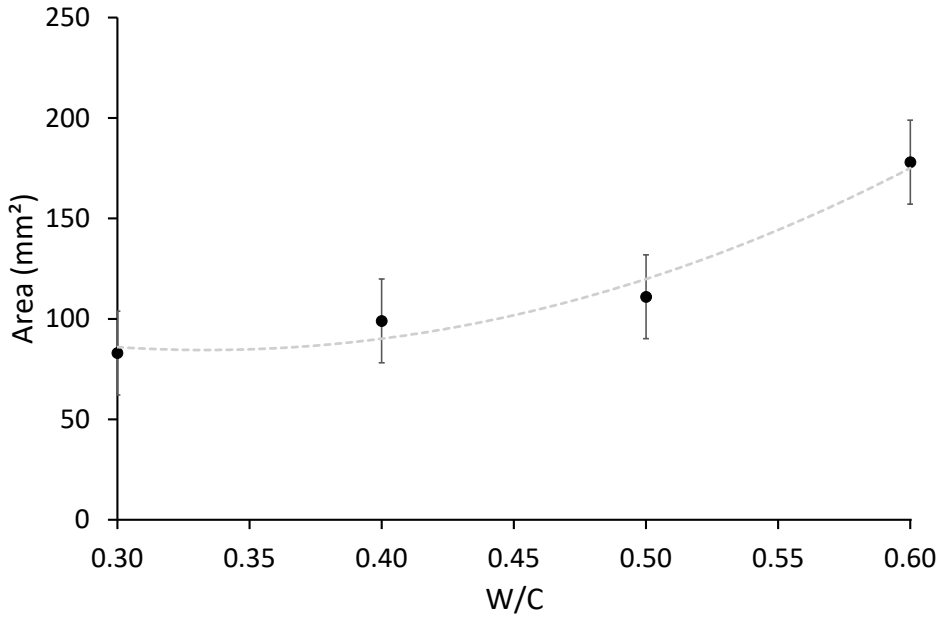

Figure 11. Evolution of the area of the ITZ as a function of W/C.

5.4 Discussion

Interfacial transition zones observed around the vegetal particles prove that the presence of plants modifies the hydration mechanisms of the mineral binder [7, 18, 19]. At a mesoscopic scale, biobased concrete could be considered as a three phases composite material constituted by hardened binder paste, vegetal aggregates, and an ITZ between those two. Therefore, the observation and the quantification of ITZ have been carried out to prevent incompatibility issues between binders and vegetal aggregates. An experimental protocol has been developed to evaluate the ITZ for hemp-cement concretes. However, the results of observations or monitoring of ITZ formation with time are still widely dispersed. They concern only the measurement of the modified area around the particles and the gradient of chemical properties of this phase, and not its microstructure and mechanical properties.

6 Conclusions

Hempcrete, which is a mixture of a cement and/or lime binder and vegetal particles, is a good insulation material, presenting advantageous hygrothermal and acoustic properties. However, the mechanical properties of hempcrete are poorer than some other materials because the Interfacial Transition Zone (ITZ) around the hemp particles is not hydrated like the rest of the matrix. It is therefore necessary to be able to quantify and analyze hydration in this zone. An

experimental test, based on image analysis, was developed to achieve a repetitive and robust visual observation of the formation of the ITZ.

From the presented studies the following conclusions can be drawn:

(1) The protocol developed is easily reproducible and robust, and can be used to test different binders or hemp treatments to obtain reliable and regular results.

(2) The chemical and microstructural analyses performed concerning the differences between the ITZ and the rest of the matrix are coherent and reliable. Regarding the influence of the W/C ratio, the less viscous the paste is, the easier the extracts can diffuse, creating a larger ITZ.

(3) W/C ratios of 0.3 and 0.6 are the limits of the protocol proposed, for the binder used – namely Portland cement. The overnight acquisition was also a significant improvement, helping to understand the kinetics of the halo formation. The ITZ forms from its outer edges and expands toward the pellet. The area of the ITZ is therefore set at the earlier stages of hydration, around 5 hours after pouring.

(4) The origin of this phenomenon was highlighted by the microstructural analyses, all of which reached the same conclusion: the ITZ is an unhydrated zone of the matrix due to the presence of hemp and its extractible components (sugars and other extracts). Indeed, lower portlandite content was found in the samples taken from the ITZ where anhydrous components like C3S were found in the majority.

Future investigations will focus on the interaction and percolation of the ITZ, placing several hemp shiv pellets on the glass at varying distances from each other. Preliminary tests have also been performed with a pre-wet pellet, thicker pellet or pellets using a water-retention agent (Diutan Gum) to avoid bleeding. However, further study is still needed to achieve reliable results. The goal will be to correlate the results of this new test on a small scale with the mechanical and thermal performances of the hemp concrete samples.

7 Acknowledgements

The authors acknowledge the support of the French Agence Nationale de la Recherche (ANR), under grant ANR-21-CE22-0009 (project BIO-UP).

8 References

[1] C. Niyigena, S. Amziane, A. Chateauneuf, Multicriteria analysis demonstrating the impact of shiv on the properties of hemp concrete, Constr. Build. Mater. 160 (2018) 211–222. doi:10.1016/j.conbuildmat.2017.11.026

[2] B Szostak, GL Golewski. Potential of siliceous fly ash and silica fume as a substitute for binder in cementitious concretes (2018), IOP Conf. Ser.: Mater. Sci. Eng. 416 012105

[3] DM. Gil and GL. Golewski. E3S Web Conf., 49 (2018) 00030. DOI: https://doi.org/10.1051/e3sconf/20184900030

[4] B. Szostak, GL. Golewski. Rheology of Cement Pastes with Siliceous Fly Ash and the CSH Nano-Admixture. Materials (2021), 14, 3640. https://doi.org/10.3390/ma14133640

[5] GL Golewski, B. Szostak. Application of the C-S-H Phase Nucleating Agents to Improve the Performance of Sustainable Concrete Composites Containing Fly Ash for Use in the Precast Concrete Industry. Materials, Basel (2021) Oct 29;14(21):6514. doi: 10.3390/ma14216514

[6] GL. Golewski, B. Szostak. Strengthening the very early-age structure of cementitious composites with coal fly ash via incorporating a novel nanoadmixture based on C-S-H phase activators, Construction and Building Materials, 312 (2021), 125426, ISSN 0950-0618, https://doi.org/10.1016/j.conbuildmat.2021.125426

[7] Y. Diquélou, E. Gourlay, L. Arnaud, B. Kurek, Impact of hemp shiv on cement setting and hardening: Influence of the extracted components from the aggregates and study of the interfaces with the inorganic matrix, Cem. Concr. Comp. 55 (2015) 112–121. doi:10.1016/j.cemconcomp.2014.09.004.

[8] E. Gourlay, P. Glé, S. Marceau, C. Foy, S. Moscardelli. Effect of water content on the acoustical and thermal properties of hemp Concretes. Constr. Build. Mater. 139 (2017) 513–523.

[9] F. Collet, S. Pretot, Experimental investigation of moisture buffering capacity of sprayed hemp concrete, Constr. Build. Mater. 36 (2012) 58-65. doi.org/10.1016/j.conbuildmat.2012.04.139

[10] M.P. Boutin, *Étude des caractéristiques environnementales du chanvre par l'analyse de son cycle de vie*. Ministère de l'agriculture et de la pêche (2006).

[11] G. Delannoy, S. Marceau, P. Glé, E. Gourlay, M. Guéguen-Minerbe, D. Diafi, S. Amziane, F. Farcas, Impact of hemp shiv extractives on hydration of Portland cement, Constr. Build. Mater. 244 (2020) 118300. doi:10.1016/j.conbuildmat.2020.118300.

[12] B. Na, Z. Wang, H. Wang, X. Lu, Wood-cement compatibility review, Wood Res. 59 (2014) 813–825.

[13] E. Boix, E. Gineau, J.O. Narciso, H. Höfte, G. Mouille, P. Navard, Influence of chemical treatments of miscanthus stem fragments on polysaccharide release in the presence of cement and on the mechanical properties of bio-based concrete materials, Cem. Concr. Compos. (2020). doi:10.1016/j.cemconcomp.2019.103429.

[14] A. Bourdot, C. Magniont, M. Lagouin, C. Niyigena, P. Evon, S. Amziane, Impact of Bio-Aggregates Properties on the Chemical Interactions with Mineral Binder, Application to Vegetal Concrete, J. Adv. Concr. Technol. 17 (2019) 542–558. doi:10.3151/jact.17.542.

[15] G.C.H. Doudart de la Grée, Q.L. Yu, H.J.H. Brouwers, Assessing the effect of CaSO4 content on the hydration kinetics, microstructure and mechanical properties of cements containing sugars, Constr. Build. Mater. 143 (2017) 48–60. doi:10.1016/j.conbuildmat.2017.03.067.

[16] N.B. Milestone, Hydration of Tricalcium Silicate in the Presence of Lignosulfonates, Glucose, and Sodium Gluconate, J. Am. Ceram. Soc. 62 (1979) 321–324. doi:10.1111/j.1151-2916.1979.tb19068.x

[17] V. Nozahic, S. Amziane, Influence of sunflower aggregates surface treatments on physical properties and adhesion with a mineral binder, Compos. Part A Appl. Sci. Manuf. 43 (2012) 1837–1849. doi:10.1016/j.compositesA.2012.07.011.

[18] P. Carrara, L. De Lorenzis, Consistent identification of the interfacial transition zone in simulated cement microstructures, Cem. Concr. Compos. 80 (2017) 224–234. doi:10.1016/j.cemconcomp.2017.03.008.

[19] F. Wu, Q. Yu, C. Liu, Durability of thermal insulating bio-based lightweight concrete: Understanding of heat treatment on bio-aggregates, Constr. Build. Mater. 269 (2021) 121800. doi:10.1016/j.conbuildmat.2020.121800.

[20] Amziane S., Collet F., Lawrence M., Magniont C., Picandet V., Sonebi M, Recommendation of the RILEM TC 236-BBM: characterisation testing of hemp shiv to determine the initial water content, water absorption, dry density, particle size distribution and thermal conductivity. Mater. and Str. 50 (2017) 167. doi 10.1617/s11527-017-1029-3

[21] J. Damerval, Experimental tools for particle size distribution and thermal analysis. Application to hemp. Master Research Thesis, INSA Lyon, 2020.

[22] L. Jalabert, Evaluation of the microwave impact on the adhesion between hemp fibers and a binder. Master Research Thesis, INSA Lyon, 2020.
[23] OMNIC user Guide version 7.3 (2006). Themo Electron corporation. Madison. USA.
[24] Diffrac.Suite User Manuel (2011). Bruker AXS GmbH. Karlsruhe, Germany.
[25] Labview User Manuel (2019). National Instrument. Austin, USA.
[26] M. Le Troedec, D. Sedan, C. Peyratout, J-P. Bonnet, A. Smith, R. Guinebretiere, V. Gloaguen, P. Krausz, Influence of various chemical treatments on the composition and structure of hemp fibres, Composites: Part A 39 (2008) 514–522.
[27] L. Ferrus, P. Pagés. Water retention value and degree of crystallinity by infrared absorption spectroscopy in caustic soda treated cotton. Cell. Chem. Technol. 11 (1977) 633–7.
[28] O'Connor RT, DuPré EF, Mitchman D. Applications of infrared absorption spectroscopy to investigations of cotton and modified cottons. Text. Res. J. 28 (1958) 382–92.